MICROCOPY RESOLUTION TEST CHART

NATIONAL BUREAU OF STANDARDS-1963-A

ADA038627

(12)

D D C
RECEIVED
APR 22 1977
B

ωⱼ WATKINS-JOHNSON

PYROLYTIC BORON NITRIDE AS A
DIELECTRIC SUBSTRATE MATERIAL
FOR MICROSTRIP INTEGRATED CIRCUITS

by
C.M. Krowne

Watkins-Johnson Company
Stanford Industrial Park
3333 Hillview Avenue
Palo Alto, California 94304

March 1977

FINAL REPORT

DDC

RECEIVED

APR 22 1977

B

REPORT DOCUMENTATION PAGE		READ INSTRUCTIONS BEFORE COMPLETING FORM
1. REPORT NUMBER	2. GOVT ACCESSION NO.	3. RECIPIENT'S CATALOG NUMBER
4. TITLE (and Subtitle) Pyrolytic Boron Nitride as a Dielectric Substrate Material for Microwave Integrated Circuits		5. TYPE OF REPORT & PERIOD COVERED 1 June 1976 through 1 April 1977 Final Report
		6. PERFORMING ORG. REPORT NUMBER
7. AUTHOR(s) C. M. Krowne		8. CONTRACT OR GRANT NUMBER(s) N00014-76-C-0896
9. PERFORMING ORGANIZATION NAME AND ADDRESS Watkins-Johnson Company 3333 Hillview Avenue Palo Alto, California 94304		10. PROGRAM ELEMENT, PROJECT, TASK AREA & WORK UNIT NUMBERS 43 p.
11. CONTROLLING OFFICE NAME AND ADDRESS Office of Naval Research 800 N. Quincy Street Arlington, Virginia 22217		12. REPORT DATE 1 April 1977
		13. NUMBER OF PAGES 39
14. MONITORING AGENCY NAME & ADDRESS(If different from Controlling Office) Same		15. SECURITY CLASS. (of this report) Unclassified
		15a. DECLASSIFICATION/DOWNGRADING SCHEDULE

16. DISTRIBUTION STATEMENT (of this Report)

Approved Public Release - Distribution Unlimited

Final rept. 1 Jun 76 - 1 Apr 77,

17. DISTRIBUTION STATEMENT (of the abstract entered in Block 20, if different from Report)

18. SUPPLEMENTARY NOTES

19. KEY WORDS (Continue on reverse side if necessary and identify by block number)

Propagation of microwaves in single and coupled microstrip transmission lines.
Substrates with anistropic dielectric constant
10 dB coupler optimization
Pyrolytic boron nitride as a microwave substrate material.

20. ABSTRACT (Continue on reverse side if necessary and identify by block number)

Quasi-TEM electromagnetic theory is developed for microstrip lines on diagonal tensor dielectric substrate materials. Computer programs * based on this theory using method of moments are described and were utilized to determine the electrical parameters for single and parallel-coupled microstrip lines on the substrate material pyrolytic boron nitride (PBN). Experimental measurements for single lines on PBN and for quadrature interdigitated coupled lines on PBN are reported.

* Computer programs utilized to perform under this contract were not developed under this contract.

DD FORM 1473 1 JAN 73   EDITION OF 1 NOV 65 IS OBSOLETE

INSTRUCTIONS FOR PREPARATION OF REPORT DOCUMENTATION PAGE

RESPONSIBILITY. The controlling DoD office will be responsible for completion of the Report Documentation Page, DD Form 1473, in all technical reports prepared by or for DoD organizations.

CLASSIFICATION. Since this Report Documentation Page, DD Form 1473, is used in preparing announcements, bibliographies, and data banks, it should be unclassified if possible. If a classification is required, identify the classified items on the page by the appropriate symbol.

COMPLETION GUIDE

General. Make Blocks 1, 4, 5, 6, 7, 11, 13, 15, and 16 agree with the corresponding information on the report cover. Leave Blocks 2 and 3 blank.

Block 1. Report Number. Enter the unique alphanumeric report number shown on the cover.

Block 2. Government Accession No. Leave Blank. This space is for use by the Defense Documentation Center.

Block 3. Recipient's Catalog Number. Leave blank. This space is for the use of the report recipient to assist in future retrieval of the document.

Block 4. Title and Subtitle. Enter the title in all capital letters exactly as it appears on the publication. Titles should be unclassified whenever possible. Write out the English equivalent for Greek letters and mathematical symbols in the title (see *"Abstracting Scientific and Technical Reports of Defense-sponsored RDT/E,"AD-667 000*). If the report has a subtitle, this subtitle should follow the main title, be separated by a comma or semicolon if appropriate, and be initially capitalized. If a publication has a title in a foreign language, translate the title into English and follow the English translation with the title in the original language. Make every effort to simplify the title before publication.

Block 5. Type of Report and Period Covered. Indicate here whether report is interim, final, etc., and, if applicable, inclusive dates of period covered, such as the life of a contract covered in a final contractor report.

Block 6. Performing Organization Report Number. Only numbers other than the official report number shown in Block 1, such as series numbers for in-house reports or a contractor/grantee number assigned by him, will be placed in this space. If no such numbers are used, leave this space blank.

Block 7. Author(s). Include corresponding information from the report cover. Give the name(s) of the author(s) in conventional order (for example, John R. Doe or, if author prefers, J. Robert Doe). In addition, list the affiliation of an author if it differs from that of the performing organization.

Block 8. Contract or Grant Number(s). For a contractor or grantee report, enter the complete contract or grant number(s) under which the work reported was accomplished. Leave blank in in-house reports.

Block 9. Performing Organization Name and Address. For in-house reports enter the name and address, including office symbol, of the performing activity. For contractor or grantee reports enter the name and address of the contractor or grantee who prepared the report and identify the appropriate corporate division, school, laboratory, etc., of the author. List city, state, and ZIP Code.

Block 10. Program Element, Project, Task Area, and Work Unit Numbers. Enter here the number code from the applicable Department of Defense form, such as the DD Form 1498, "Research and Technology Work Unit Summary" or the DD Form 1634, "Research and Development Planning Summary," which identifies the program element, project, task area, and work unit or equivalent under which the work was authorized.

Block 11. Controlling Office Name and Address. Enter the full, official name and address, including office symbol, of the controlling office. (Equates to funding/sponsoring agency. For definition see DoD Directive 5200.20, "Distribution Statements on Technical Documents.")

Block 12. Report Date. Enter here the day, month, and year or month and year as shown on the cover.

Block 13. Number of Pages. Enter the total number of pages.

Block 14. Monitoring Agency Name and Address (if different from Controlling Office). For use when the controlling or funding office does not directly administer a project, contract, or grant, but delegates the administrative responsibility to another organization.

Blocks 15 & 15a. Security Classification of the Report: Declassification/Downgrading Schedule of the Report. Enter in 15 the highest classification of the report. If appropriate, enter in 15a the declassification/downgrading schedule of the report, using the abbreviations for declassification/downgrading schedules listed in paragraph 4-207 of DoD 5200.1-R.

Block 16. Distribution Statement of the Report. Insert here the applicable distribution statement of the report from DoD Directive 5200.20, "Distribution Statements on Technical Documents."

Block 17. Distribution Statement (of the abstract entered in Block 20, if different from the distribution statement of the report). Insert here the applicable distribution statement of the abstract from DoD Directive 5200.20, "Distribution Statements on Technical Documents."

Block 18. Supplementary Notes. Enter information not included elsewhere but useful, such as: Prepared in cooperation with . . . Translation of (or by) . . . Presented at conference of . . . To be published in . . .

Block 19. Key Words. Select terms or short phrases that identify the principal subjects covered in the report, and are sufficiently specific and precise to be used as index entries for cataloging, conforming to standard terminology. The DoD "Thesaurus of Engineering and Scientific Terms" (TEST), AD-672 000, can be helpful.

Block 20. Abstract. The abstract should be a brief (not to exceed 200 words) factual summary of the most significant information contained in the report. If possible, the abstract of a classified report should be unclassified and the abstract to an unclassified report should consist of publicly-releasable information. If the report contains a significant bibliography or literature survey, mention it here. For information on preparing abstracts see "Abstracting Scientific and Technical Reports of Defense-Sponsored RDT&E," AD-667 000.

TABLE OF CONTENTS

1. INTRODUCTION

The motivation for using pyrolytic boron nitride (PBN)[1] as a substrate is that by proper choices of microstrip coupled line parameters the difference d between the odd (v_{po}) and even (v_{pe}) mode phase velocities may be made very small in comparison to other commonly used isotropic (or nearly so) substrate materials. d is given by

$$d = 100 \frac{v_{po} - v_{pe}}{\bar{v}} \tag{1}$$

where $\bar{v}$ is the average mode phase velocity. Coupled line microstrip structures built on PBN such as couplers and edge-coupled filters would have low d values resulting in less unwanted microwave signal distortion. In couplers, this low d value should result in both less signal distortion and greater directivity compared to other substrate materials used in the microstrip configuration. Directivity here refers to the power output of the isolated port (P_i) relative to the indirect output port (P_{id}) (Figure 1).

It is the anisotropic nature of the PBN permittivity tensor $\bar{\bar{\epsilon}}$ which allows d to be reduced markedly in comparison to other commonly used substrate materials such as alumina and fused silica which give d values typically between 6.7% and 8.7%. PBN has a crystalline structure with layered atomic planes in the x z-plane (the x and z directions are referred to as "a" directions) normal to the y-axis (referred to as the "c" direction). See Figure 2 for a diagram of the crystalline geometry. In the xz-plane the relative permittivity is $\epsilon_x = \epsilon_z = 5.12$ and normal to this plane $\epsilon_y = 3.4$.

Figure 3 shows a schematic cross-section of a coupled microstrip line structure. The PBN crystal is oriented so that the "a" axes lie parallel to the ground plane. The "c" axis is perpendicular to the ground plane. H, t, S, and w are respectively the PBN substrate thickness, the microstrip conductor line thickness, the edge-to-edge spacing between the coupled lines, and the width of the lines. The configuration in Figure 3 is idealized since the ground plane walls on the sides of the substrate and above it are absent. In this uncovered microstrip structure the electromagnetic field lines are found both in the dielectric substrate and in the medium (air) above the dielectric. Two different types of propagating waves flow down the lines: the even and odd modes. The even mode is that electromagnetic

ISOLATED   DIRECT OUTPUT

P_i

50Ω P_d

INPUT

P_{in} INDIRECT OUTPUT
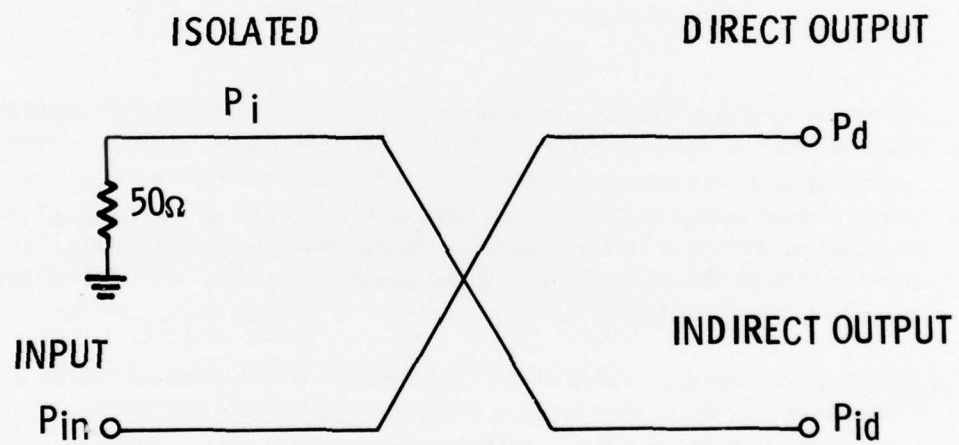
                                    P_{id}

Figure 1: Schematic diagram of a quadrature coupler.
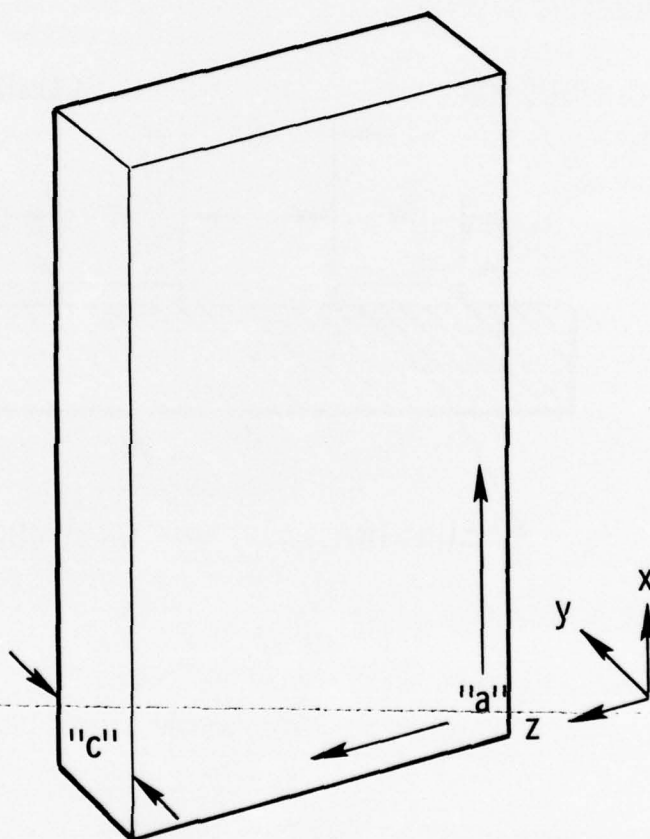The coupler is in the 50Ω system.

Figure 2: Crystalline structure of pyrolytic boron nitride (PBN).
PBN has layered atomic planes parallel to the "a"
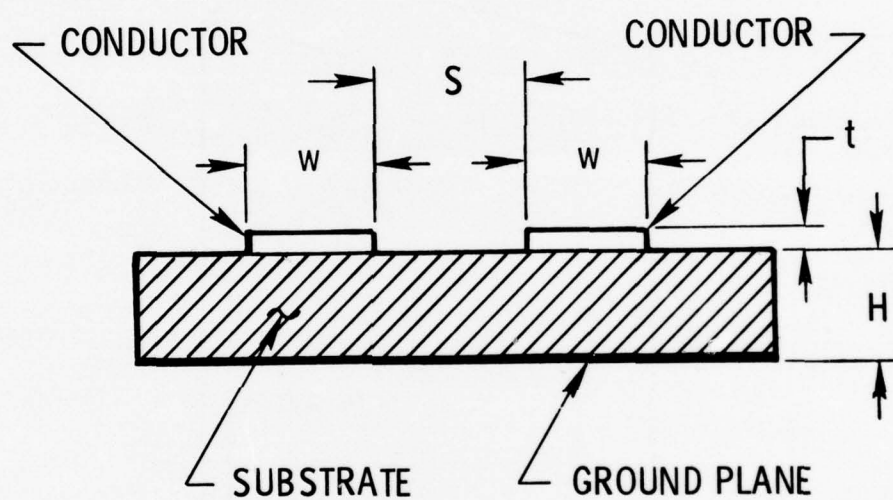direction normal to the "c" crystalligraphic direction.

- 3 -

Figure 3: Cross-section of simple uncovered coupled microstrip lines.

field solution corresponding to like charges residing on the two coupled lines. The odd mode corresponds to opposite charges. The electric field lines are shown in Figure 4 for the structure in Figure 3. The odd mode allows a much greater amount of field lines to pass through the air in comparison to the even mode. The net result of this difference in electric field distribution is that the odd mode will effectively see a significantly lower dielectric constant ϵ_o than the even mode ϵ_e if the dielectric substrate is isotropic and if the substrate dielectric constant ϵ_s is substantially larger than air as it is for a number of commonly used substrates such as alumina and fused silica ($\epsilon_{alumina} \sim 9.8$; $\epsilon_{fused\ silica} \sim 3.8$).

Both the even and odd modes may be characterized as transverse electromagnetic (TEM) solutions with their phase velocities of propagation $v_p \sim \epsilon^{-1/2}$. Since ϵ_o and ϵ_e are significantly different for isotropic substrates, there will be a substantial phase velocity discrepancy or difference d between the even and odd modes. This v_p discrepancy creates a phase imbalance in the coupler which limits its directivity. However, if an anisotropic substrate is used which has one dielectric constant $\epsilon_a = \epsilon_x = \epsilon_z$ parallel to the ground plane and another ϵ_y normal to this plane such that $\epsilon_y > \epsilon_a$, the mismatch between the phase velocities can be reduced. This is the case for PBN if the a-axes are placed parallel to the ground plane since this will cause $\epsilon_a = 5.12$ and $\epsilon_y = 3.4$.

A qualitative argument will show that PBN in the above orientation reduces the difference between ϵ_o and ϵ_e and therefore the phase velocity difference d. The even mode effective dielectric constant should be close to ϵ_y since most of the electric field lines lie between the microstrip conductor lines and the ground plane (Figure 4). Thus $\epsilon_e \approx 3.4$. On the other hand, the odd mode has field lines between (1) the microstrip and the ground plane, and (2) between the microstrip lines in air and the substrate. One can very roughly estimate what ϵ_o might be by averaging the ϵ's parallel to the ground plane as
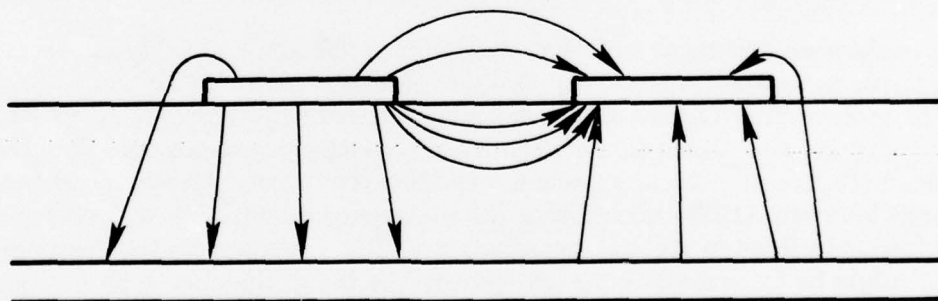
$$\epsilon_p = \frac{1.0 + 5.12}{2}$$

$$= 3.06$$

and finding the average of ϵ_p and ϵ_y:

$$\epsilon_o \approx \frac{3.06 + 3.4}{2}$$

$$= 3.23.$$
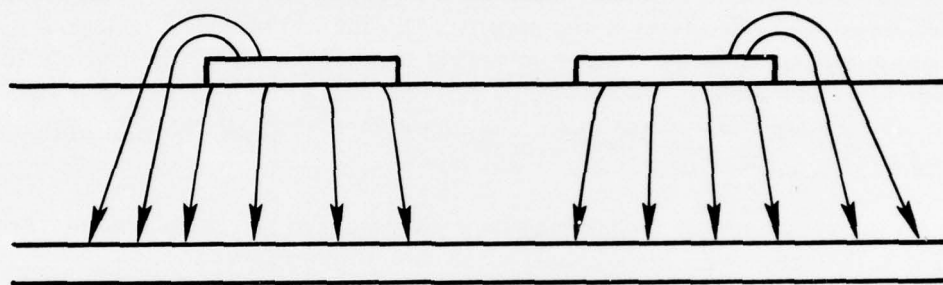
(a) Even Mode

(b) Odd Mode

Figure 4: Cross sectional views of the Even (a) and Odd (b) Mode electric field distributions for uncovered coupled microstrip shown in Figure 3.

One sees that $\epsilon_e \approx 3.4$ and $\epsilon_0 \approx 3.23$ are reasonably close implying that a rigorous solution of the microstrip coupled line problem could indeed yield zeros for d.

The uncovered microstrip structure of Figure 3 can be compared to the conductor line configuration seen in the parallel coupled stripline of Figure 5. The conductor lines are immersed in one dielectric (chosen to be isotropic) so that the effective dielectric constants seen by the even and odd modes are equal. Notice that the lines are symmetrically sandwiched by the dielectric material and the two conducting ground planes. This geometric disposition of the lines leads to a homogeneous boundary value problem for electromagnetic waves propagating down the lines. In contrast, the microstrip line geometry seen in Figure 3 for the simple case of an isotropic dielectric constitutes an inhomogeneous boundary value problem for electromagnetic waves. In the next section we shall solve this inhomogeneous boundary value problem for an anisotropic dielectric substrate having a diagonal relative dielectric tensor.
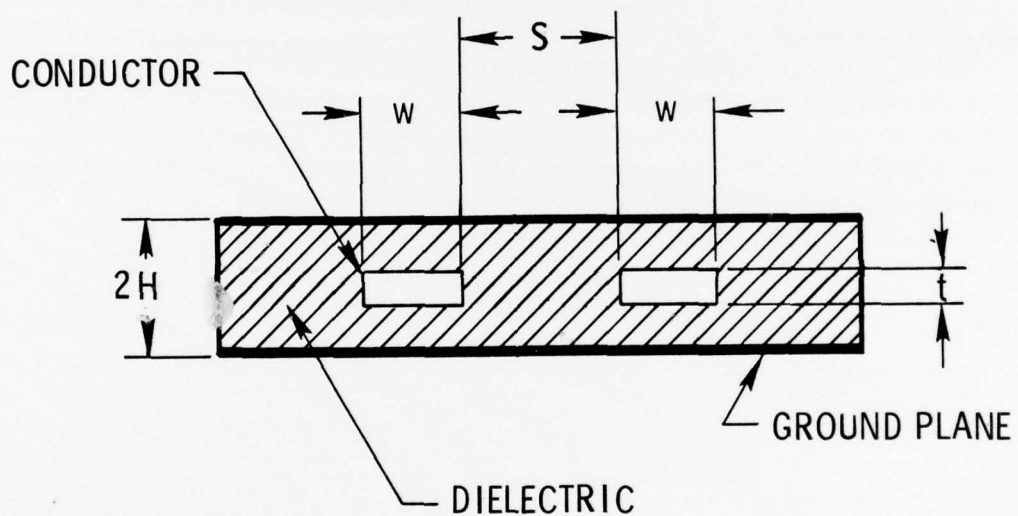
Figure 5: Cross-sectional view of a stripline configuration where the parallel coupled lines are parallel to the ground planes and equidistant between them.

2. INHOMOGENEOUS BOUNDARY VALUE PROBLEM FOR AN ANISOTROPIC SUBSTRATE

Here will we determine the Green's function for a single microstrip line in the covered configuration shown in Figure 6. This configuration is very convenient for solving the boundary value problem. As before, we define the y-axis perpendicular to the ground planes with the x-axis in the plane of the paper and parallel to the ground planes and the z-axis perpendicular to the plane of paper. The medium above the anisotropic substrate is taken to be isotropic with a relative dielectric constant of

$$\epsilon_2 = n_2^2 \qquad (2)$$

where n_2 is the refractive index of the medium. For the anisotropic medium ϵ_x and ϵ_y are two of the orthogonal components of the dielectric constant tensor. We take $\epsilon_x = \epsilon_z$ so that the components in the x and z directions are degenerate. The y component ϵ_y is such that $\epsilon_y \neq \epsilon_x$. We define the refractive indexes n_y and n_x so that

$$\epsilon_x = n_x^2 \quad , \qquad (3)$$

$$\epsilon_y = n_y^2 \quad . \qquad (4)$$

In Figure 6, B is the ground-plane to ground-plane separation. For our approach we set the conductor line thickness t (seen in Figure 3) equal to zero.

Once the Green's function has been determined for a single microstrip line, the coupled microstrip line problem is also solved since the same form of Green's function must be utilized. Employing a method of moments computation technique which is standard in the literature allows coupled line electrical parameters to be calculated.[2] These parameters include the even and odd mode capacitances, phase velocities, and characteristic line impedances. Figure 7 shows the covered parallel coupled microstrip cross-sectional geometry where in the general case the line widths w_1 and w_2 are $w_1 \neq w_2$.
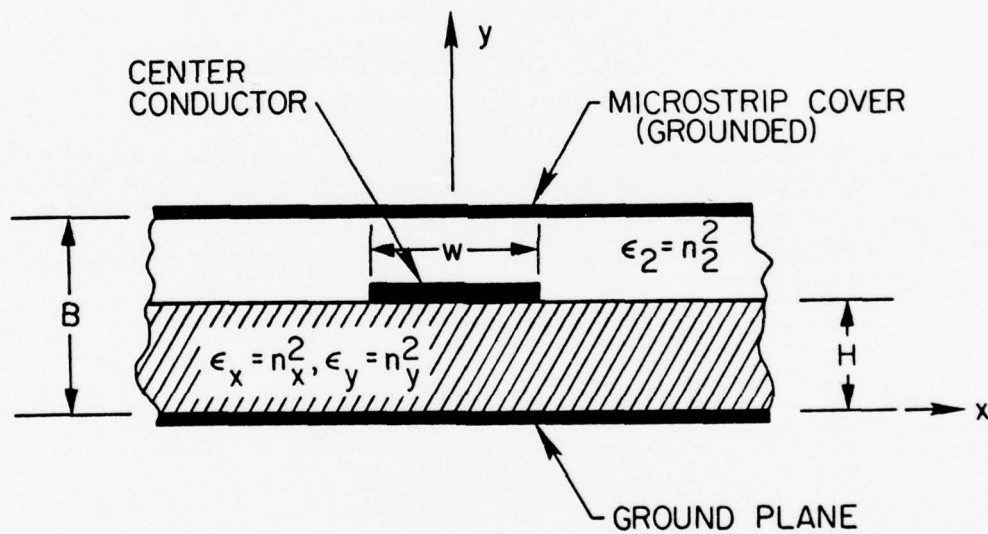
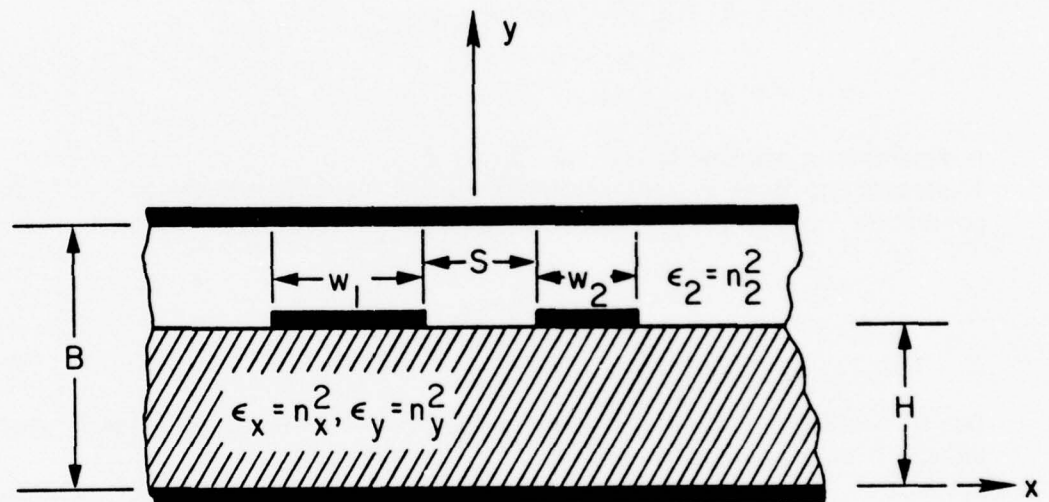Figure 6: Cross-section of a single covered microstrip line above an anisotropic substrate dielectric.

Figure 7: Cross-section of covered parallel coupled microstrip
lines on an anisotropic dielectric substrate.

- 11 -

Consider the single line in Figure 6 where the line has unity coulombs per meter of charge and runs parallel to the z-axis. Then the permittivities of the medium above the substrate (ϵ) and of the anisotropic substrate ($\bar{\bar{\epsilon}}$) are given based on the above discussion, respectively, by

$$\epsilon = \epsilon_2 \quad , \quad H < y < B \ ; \tag{5}$$

$$\bar{\bar{\epsilon}} = \begin{pmatrix} \epsilon_x & 0 & 0 \\ 0 & \epsilon_y & 0 \\ 0 & 0 & \epsilon_x \end{pmatrix} , \quad 0 < y < H \ . \tag{6}$$

A quasi-static solution to the potential problem can be obtained by solving Laplace's equations in the two dielectric regions subject to the proper boundary conditions. One needs to solve in the anisotropic region the equation

$$\nabla \cdot (\bar{\bar{\epsilon}} \cdot \nabla \phi_1) = 0 \quad . \tag{7}$$

Due to the infinite extent of the line in the z direction, the problem is two dimensional. Therefore Eq. (7) yields

$$\epsilon_x \frac{\partial^2 \phi_1}{\partial x^2} + \epsilon_y \frac{\partial^2 \phi_1}{\partial y^2} = 0 \tag{8}$$

which has a solution of the form

$$\phi_1(x,y) = \left[a_1(k) \cos\left(\frac{kx}{n_x}\right) + b_1(k) \sin\left(\frac{kx}{n_x}\right) \right] \left[c_1(k) \sinh\left(\frac{ky}{n_y}\right) + d_1(k) \cosh\left(\frac{ky}{n_y}\right) \right] \tag{9}$$

with k being a continuous variable. Because of the even symmetry in x and the fact that at the ground plane $\phi_1(x, 0) = 0$, it follows that the general solution of Eq. (8) can be written as

$$\phi_1(k) = \int_{-\infty}^{\infty} A_1(k) \cos\left(\frac{kx}{n_x}\right) \left\{ \frac{\sinh\left(\frac{ky}{n_y}\right)}{\sinh\left(\frac{kH}{n_y}\right)} \right\} dk \tag{10}$$

where $n_x = (\epsilon_x)^{1/2}$ and $n_y = (\epsilon_y)^{1/2}$. Using Laplace's equation in the isotropic region $(H < y < B)$, i.e.

$$\nabla^2 \phi_2 = 0 \quad , \tag{11}$$

one must obtain $\phi_2(x,y)$ such that $\phi_2(x, B) = 0$ at the top ground plane.

Normalizing the x and y variables in Eq. (11) to the same constant n_x, a general solution in region 2 is obtained in the form:

$$\phi_2(x,y) = \int_{-\infty}^{\infty} A_2(k) \cos\left(\frac{kx}{n_x}\right) \left\{ \frac{\sinh\left(\frac{k(B-y)}{n_x}\right)}{\sinh\left(\frac{k(B-H)}{n_x}\right)} \right\} dk \quad . \tag{12}$$

The electric fields in the substrate region (region 1) and above it (region 2) must at their interface $(y = H)$ satisfy continuity of the tangential electric field components and continuity of the normal electric displacement vector components $(\overline{D}_1$ and $\overline{D}_2)$. These boundary conditions may be stated, respectively, as

$$\frac{\partial \phi_1(x,y)}{\partial x}\bigg|_{y=H^-} = \frac{\partial \phi_2(x,y)}{\partial x}\bigg|_{y=H^+} \tag{13}$$

and

$$\hat{y} \cdot (\overline{D}_1 - \overline{D}_2) = -\delta(x) \quad . \tag{14}$$

- 13 -

Notice that D field continuity is broken at $x = 0$ $(y = H)$ since we encounter the line charge represented by $\delta(x)$. In Eq. (14);

$$\overline{D}_1 = \overline{D}_1(x,y)\bigg|_{y=H^-} \quad , \tag{15}$$

and

$$\overline{D}_2 = \overline{D}_2(x,y)\bigg|_{y=H^+} \quad . \tag{16}$$

Also

$$\overline{D}_1 = \overline{\overline{\epsilon}}\,\epsilon_0 \cdot \overline{E}_1$$

$$= -\overline{\overline{\epsilon}}\,\epsilon_0 \cdot \nabla\phi_1 \quad , \tag{17}$$

and

$$\overline{D}_2 = \epsilon_2\,\epsilon_0\,\overline{E}_2$$

$$= -\epsilon_2\,\epsilon_0\,\nabla\phi_2 \quad . \tag{18}$$

Here ϵ_0 is the permittivity of a vacuum.

From the continuity of potentials at $y = H$ (Eq. (13)), it follows that $A_1(k) = A_2(k) = A(k)$. By employing the boundary condition at $y = H$ which is expressed in Eq. (13), it follows that

$$\delta(x) = \int_{-\infty}^{\infty} A(k) \cos\left(\frac{kx}{n_x}\right)\left\{ n_y \coth\left(\frac{kH}{n_y}\right) + \frac{n_2^2}{n_x} \coth\left[\frac{k(B-H)}{n_x}\right] \right\} k\,dk \quad . \tag{19}$$

- 14 -

Since

$$\int_{-\infty}^{\infty} \cos\left(\frac{kx}{n_x}\right) dk = 2\pi \delta\left(\frac{x}{n_y}\right) = 2\pi\, n_x\, \delta(x) \qquad , \qquad (20)$$

$A(k)$ is obtained from Eq. (19) in the form:

$$A(k) = \frac{1}{2\pi\epsilon_0} \cdot \left\{ \frac{1}{k} \left(\frac{1}{n_x n_y \coth\left(\frac{kH}{n_y}\right) + n_2^2 \coth\left[\frac{k(B-H)}{n_x}\right]} \right) \right\} \qquad . \qquad (21)$$

The potential is now given by

$$\phi_1(x,y) = \frac{1}{2\pi\epsilon_0} \int_{-\infty}^{\infty} \frac{dk}{k} \frac{\cos\left(\frac{kx}{n_x}\right) \sinh\left(\frac{ky}{n_y}\right)}{\left\{ n_x n_y \cosh\left(\frac{kH}{n_y}\right) + n_2^2 \sinh\left(\frac{kH}{n_y}\right) \coth\left[\frac{k(B-H)}{n_x}\right] \right\}} \qquad (22)$$

for $0 \le y \le H$, and by

$$\phi_2(x,y) = \frac{1}{2\pi\epsilon_0} \int_{-\infty}^{\infty} \frac{dk}{k} \frac{\cos\left(\frac{kx}{n_x}\right) \sinh\left[\frac{k(B-y)}{n_x}\right]}{\left\{ n_x n_y \sinh\left[\frac{k(B-H)}{n_x}\right] \coth\left(\frac{kH}{n_y}\right) + n_2^2 \cosh\left[\frac{k(B-H)}{n_x}\right] \right\}}$$

$$(23)$$

for $H \le y \le B$.

If we set $y = H$ in either Eqs. (22) or (23), the Green's function for the microstrip line over an anisotropic substrate is expressed by the equation

$$\phi(x, H) = \frac{1}{2\pi\epsilon_0} \int_{-\infty}^{\infty} \frac{dk}{k} \frac{\cos\left(\frac{kx}{n_x}\right)}{\left\{n_x n_y \coth\left(\frac{kH}{n_y}\right) + n_2^2 \coth\left[\frac{k(B-H)}{n_x}\right]\right\}} \tag{24}$$

since $\phi_1(x, H) = \phi_2(x, H)$.

3. NUMERICAL APPROACH FOR STUDYING PBN

In order to compute the even and odd mode characterisitc impedances Z, phase velocities v_p, and coupling constant K parameters of coupled microstrip on PBN, a numerical approach based on the method of moments has been employed.[2] Two computer programs have been developed to compute $\phi(x, H)$ in Eq. (24). The first one evaluates Eq.(24) using a numerical integration approach.[3] This entails separating the integration interval into two ranges: Δ to P and P to ∞. If P is chosen large enough, the coth functions will approach one and the integration can be represented as follows:

$$\phi(x, H) = \frac{1}{\pi \epsilon_o} \int_\Delta^P \frac{dk}{k} \frac{\cos\left(\frac{kx}{n_x}\right)}{\left\{ n_x n_y \coth\left(\frac{kH}{n_y}\right) + n_2^2 \coth\left[\frac{k(B-H)}{n_x}\right] \right\}}$$

$$+ \frac{1}{\pi \epsilon_o \left(n_x n_y + n_2^2\right)} \int_P^\infty \frac{dk}{k} \cos\left(\frac{kx}{n_x}\right) \quad . \tag{25}$$

In order for Eq. (25) to approximate $\phi(x, H)$ well, $\Delta \rightarrow 0$ and P must be such that the coth arguments $\theta_a \gtrsim 6$. The lower limit in the first integral is not set $\Delta \equiv 0$ because the coth functions blow-up at $k = 0$, preventing a correct numerical evaluation. The second integral in Eq. (25) can be calculated using the IBM Scientific Subroutine Package program SICI.

The first integral can be determined using a Simpson integration routine. The cos argument increment $\Delta\theta_c$ must be chosen small engough to approximate the cos oscillation behavior; $\Delta\theta_c \leq 5^o$. This $\Delta\theta_c$ value specifies the k integration interval $\Delta k = n_x \Delta\theta_c / x$.

The other computer program computes $\phi(x, H)$ in Eq.(24) through a series expression Eq.(28) derived as follows. By analytic continuation $\phi(x, H)$ in Eq.(24) can be rewritten as

$$\phi(x, H) = \frac{1}{2\pi\epsilon_o} \text{Re} \oint_C \frac{dz}{z} \frac{e^{i(x/n_x) z}}{\left\{ n_x n_y \coth\left(\frac{H}{n_y} z\right) + n_2^2 \coth\left[\left(\frac{B-H}{n_x}\right) z\right] \right\}} \tag{26}$$

where z is a complex variable and C is the path of integration which extends from $-\infty$ to $+\infty$ along the $R_e(z)$ axis and closes on the upper half x plane. It can be easily demonstrated that $z = 0$ is an ordinary point and that there exists an infinite number of poles restricted to the $Im(z)$ axis. By invoking the residue theorem, $\phi(x, H)$ can be rewritten as

$$\phi(x, H) = \frac{i}{\epsilon_0} \, Re \sum_{p=1}^{\infty} Q_P \tag{27}$$

where Q_P denotes the residue at the pth pole. In accordance with this approach the residue series yields

$$\phi(x, H) = \frac{1}{\epsilon_0} \sum_{p=1}^{\infty} \frac{e^{-(|x|r_p/n_x)}}{r_p H \left[n_x \csc^2\left(\frac{Hr_p}{n_y}\right) + n_2^2 \left(\frac{\nu}{n_x}\right) \csc^2\left(\frac{H\nu}{n_x} r_p\right) \right]} \tag{28}$$

where $\nu = \dfrac{B}{H} - 1$ and r_p is the pth zero of the determinantal equation

$$\frac{\cot\left(\frac{Hr}{n_y}\right)}{\cot\left(\frac{H\nu r}{n_x}\right)} = -\frac{n_2^2}{n_x n_y} \quad . \tag{29}$$

Of interest is the special case where $n_x = n_y = n_1$; i.e., that of isotropic substrate. In this case the parameter ν is of importance in locating the roots of r_p properly. For example, if $\nu = 1$, Eq. (28) simplifies to

$$\phi(x, H) = \frac{2}{\epsilon_o} \sum_{p=1}^{\infty} \frac{e^{-(|x|/2\pi)\, p\pi}}{p\pi \left[n_1^2 + n_2^2 \right]} \qquad (30)$$

which agrees with the result obtained for isotropic substrates by Farrar and Adams.[4]

Equation (28) works most efficiently for loosely coupled microstrip lines (computer program ANIGREEN1; see Reference 5) and Eq. (25) for tightly coupled lines (computer program ANIGREEN2; see Reference 5).

4. THEORETICAL RESULTS FOR SINGLE AND COUPLED LINES ON PBN

One can calculate the electrical parameters of single and coupled microstrip lines on PBN by using, respectively, Eqs. (28) and (25).[6] For PBN, $\epsilon_x = 5.12$ and $\epsilon_y = 3.4$. Thus $n_x = 2.26$ and $n_y = 1.84$. Figure 8 shows the characteristic line impedance Z against w/H for a single line on PBN. As expected, Z decreases with increasing w/H. The result is for the cover-ground-plane to substrate-ground-plane distance B/H = 6. The difference between B/H = 6 and B/H = ∞ is at most a few percent. Figure 9 gives the phase velocity v_p normalized to the speed of light c in a vacuum against w/H. v_p/c decreases with increasing w/H, since the electric field lines are being progressively restricted to the area under the line and out of the air above the substrate.

For coupled microstrip lines, the line lengths may be different, $w_1 \neq w_2$. Below, only the results for $w_1 = w_2 = w$ are presented. Figure 10 gives the dependence of the characteristic line impedance for the odd (Z_o) and even (Z_e) modes versus w/H. Families of curves for the even and odd modes have been generated in Figure 10 by varying S/H, the edge-to-edge coupled-line-spacing/height ratio. w/H varies from 10 to 0.1 and S/H varies over an order of magnitude (0.1 to 1). The behavior of these curves is not surprising, since we expect $Z_e > Z_o$, owing to the fact that the total odd mode capacitance will exceed that seen by the even mode.

Figure 11 gives the odd v_{po} and even v_{pe} phase velocities versus w/H for a number of different S/H values. As expected, $v_{po} > v_{pe}$ for a range of w/H values (w/H > 0.7). However, for small w/H, $v_{po} > v_{pe}$ is by no means true, and as Figure 11 shows, the odd and even mode curves can cross over. This crossover point is different for different S/H. For S/H = 1, 0.5, 0.25 and 0.1, we see that the crossover, respectively, does not occur (in the w/H range), occurs at w/H = 0.22, w/H = 0.38 and at w/H = 0.65. It is at these crossover points that one expects signal distortion due to the difference between the even and odd mode phase velocities to be significantly reduced. Note that, for reasonably small w/H and S/H, the result that v_{pe} can exceed v_{po} is understandable in view of the fact that a greater proportion of the even mode fields are in air than for the odd mode.

The above results indicate that it should be possible to couple lines such that $v_{pe} \rightarrow v_{po}$ for different (w/H, S/H) combinations. Different (w/H, S/H) sets means different coupling constants K for the line-to-line coupling. K is plotted against w/H in Figure 12 for S/H = 0.1, 0.25, 0.5 and 1.0.
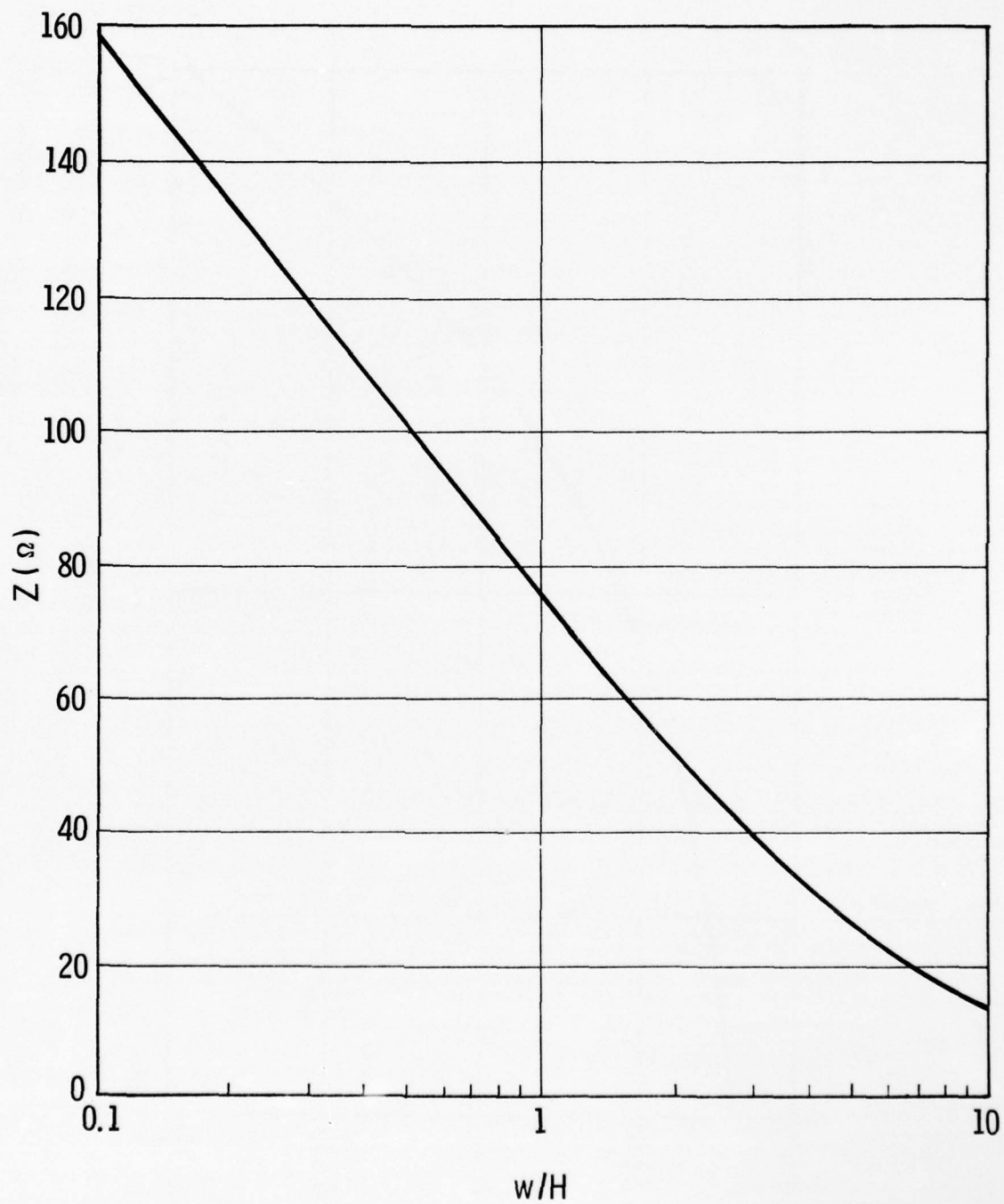
Figure 8: Z versus w/H for covered single microstrip on
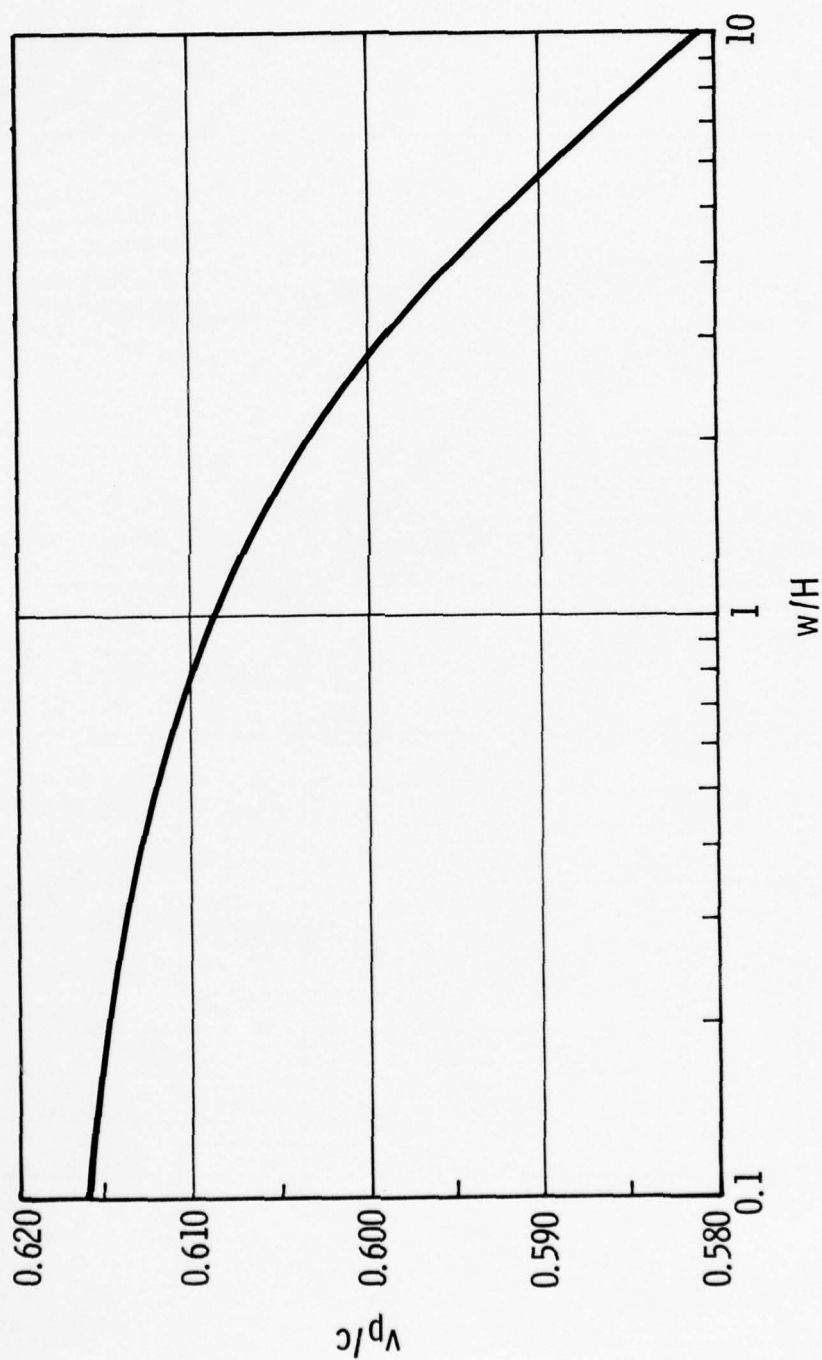pyrolytic boron nitride. B/H = 6.

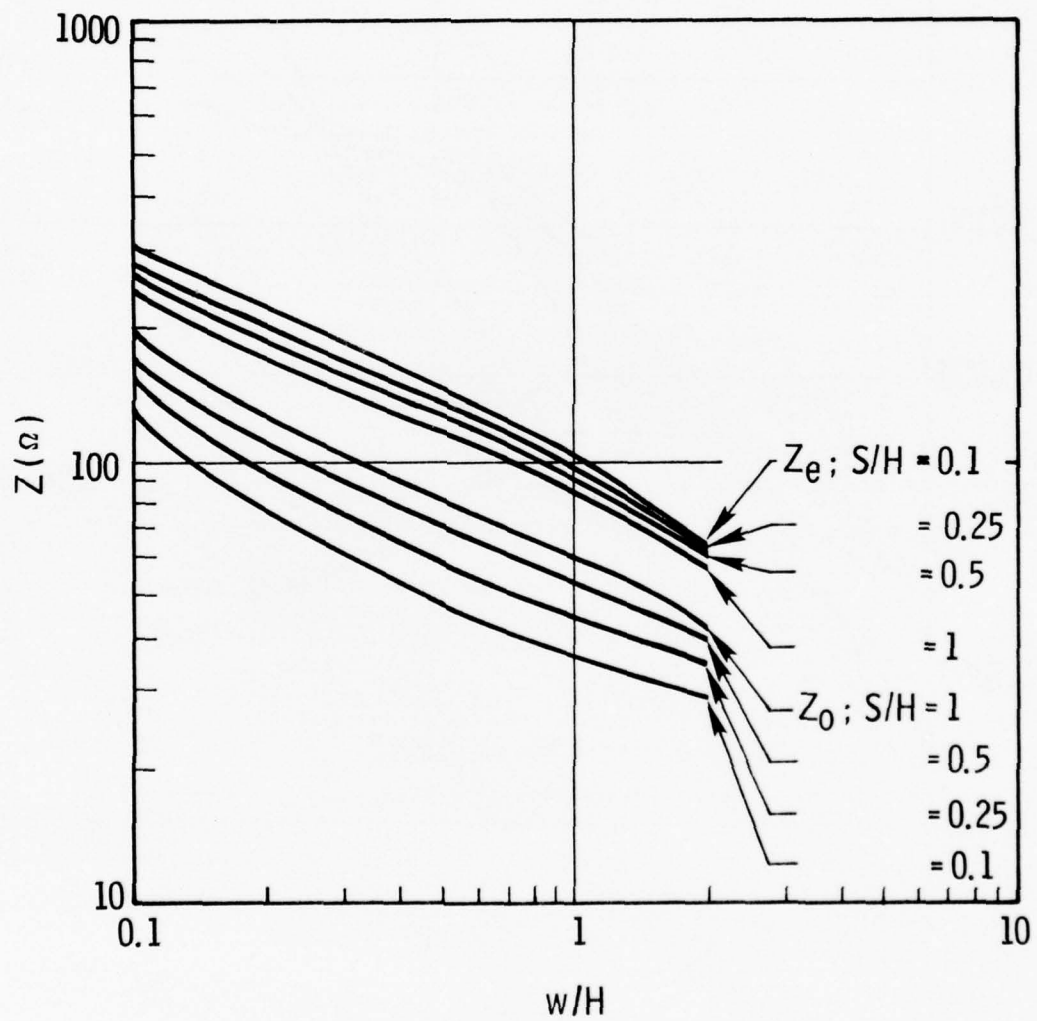Figure 9: v_p/c versus w/H for covered single microstrip on pyrolytic boron nitride. B/H = 6.

Figure 10: Z_e and Z_o versus w/H for covered parallel coupled microstrip on pyrolytic boron nitride. The family of curves has been generated for S/H = 0.1, 0.25, 0.5, and 1.0. B/H = 20.
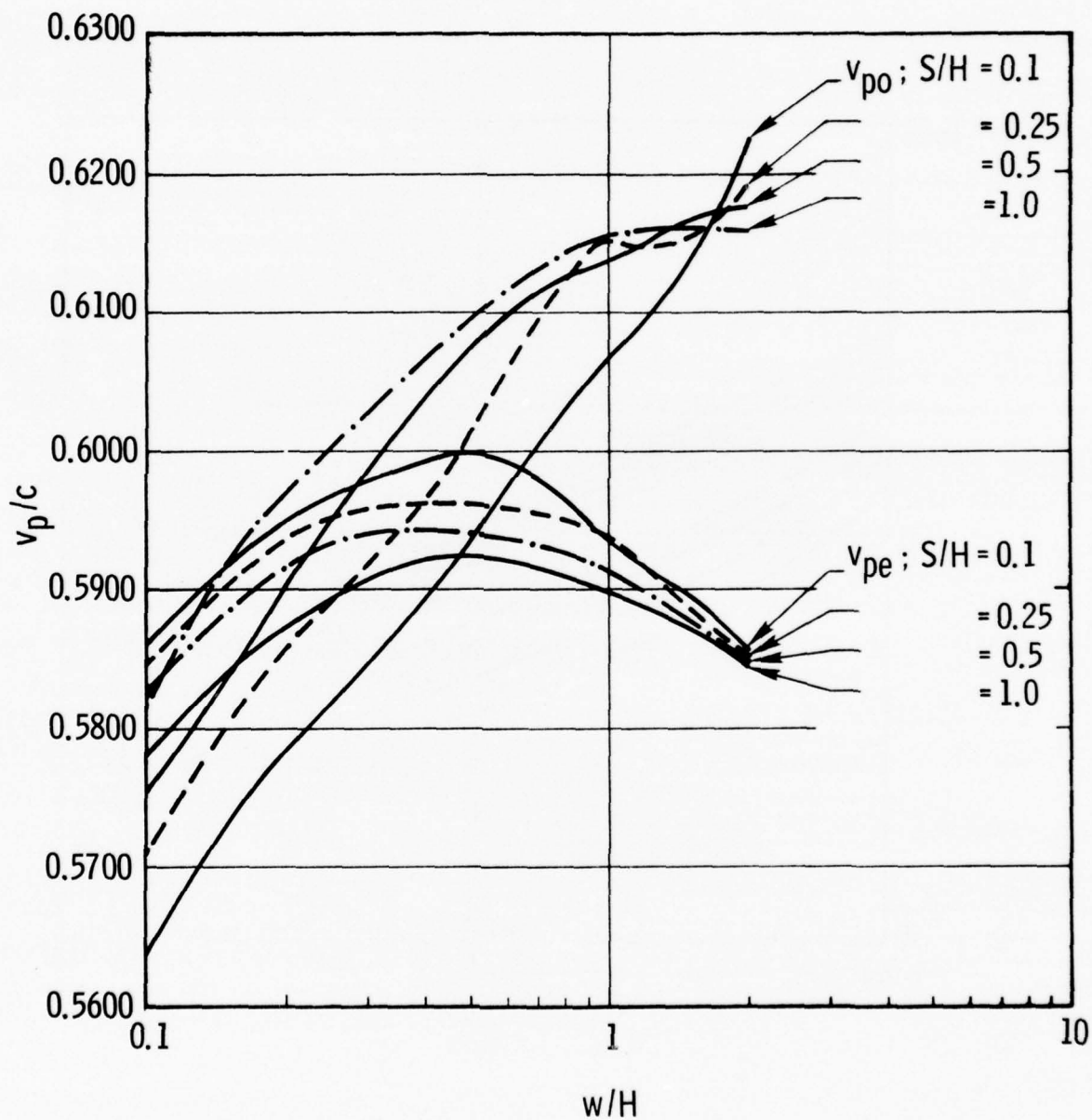
Figure 11: v_{po}/c and v_{pe}/c versus w/H for covered parallel coupled microstrip on pyrolytic boron nitride. The curves have been plotted for S/H = 0.1, 0.25, 0.5, and 1.0. B/H = 20.
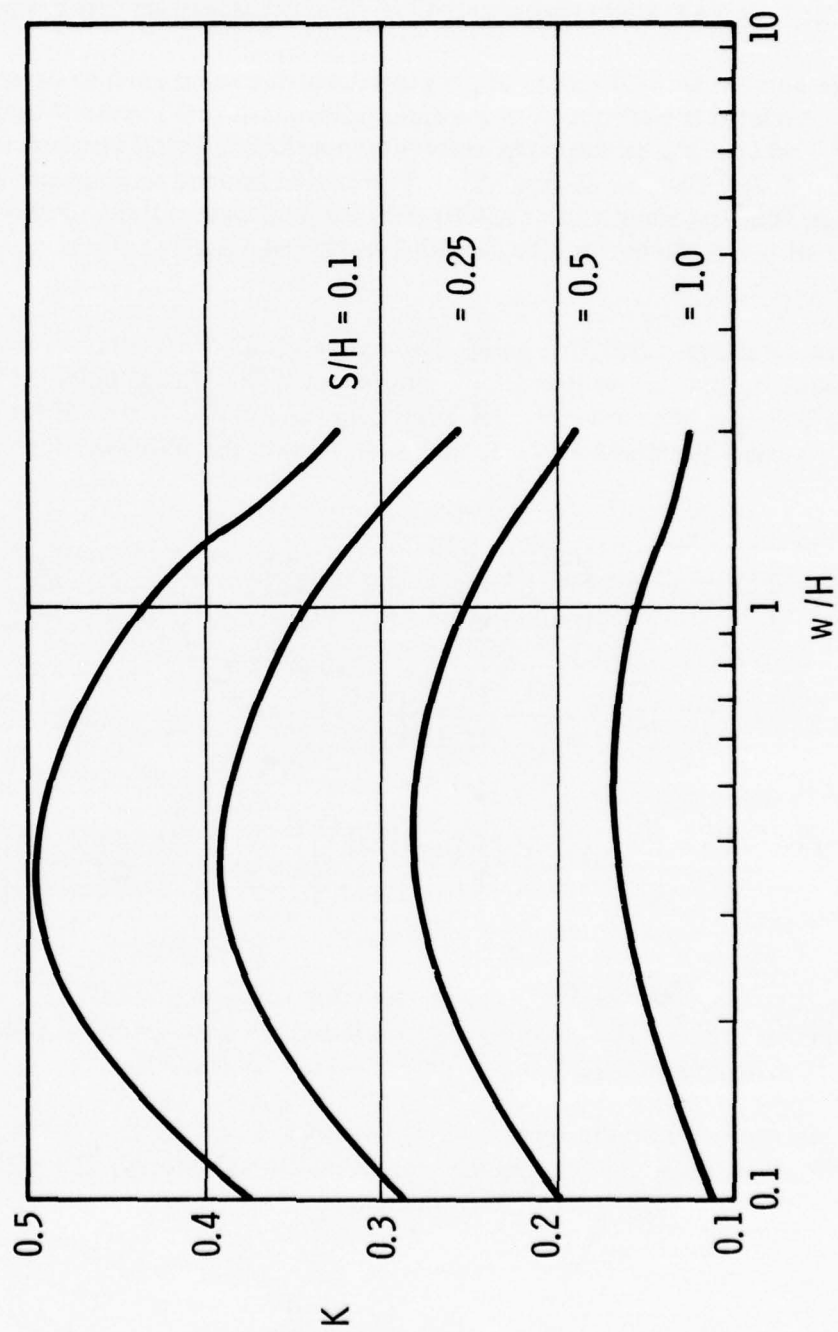
Figure 12: K versus w/H for covered parallel coupled microstrip on pyrolytic boron nitride. The curves are for varying S/H = 0.1, 0.25, 0.5, and 1.0. B/H = 20.

- 25 -

5. EXPERIMENTAL MEASUREMENTS ON SINGLE MICROSTRIP LINES ON PBN

In this section an expression is presented which can be used to determine the characteristic impedance Z of a single microstrip line provided the return loss $|\Gamma_r|^2$, where Γ_r is the input reflection coefficient being measured from a standard 50Ω line, is known. This expression is used to compare experimental voltage standing wave ratio (VSWR) data for microstrip lines on the substrate material pyrolytic boron nitride with theoretical VSWR predictions based on Z found in Figure 8.

Figure 13 shows a 50Ω line going into another impedance line Z_1 at junction 1, into another line Z_2 at junction 2, into another line Z_3 at junction 3, and back into a 50Ω line at junction 4. By adding up the infinite series of internal reflections between junctions 1, 2, 3, and 4, we obtain the following formula for $|\Gamma_r|^2$:

$$|\Gamma_r|^2 = \left[|\Gamma_1|^2 + \frac{(1 - |\Gamma_1|^2)|\Gamma_2|^2}{1 - |\Gamma_1|^2|\Gamma_2|^2} \right] + \left[1 - |\Gamma_2|^2 - \frac{(1 - |\Gamma_2|^2)|\Gamma_1|^2}{1 - |\Gamma_1|^2|\Gamma_2|^2} \right]$$

$$\times \left[1 - |\Gamma_1|^2 - \frac{(1 - |\Gamma_1|^2)|\Gamma_2|^2}{1 - |\Gamma_1|^2|\Gamma_2|^2} \right] \left[|\Gamma_3|^2 + \frac{(1 - |\Gamma_3|^2)|\Gamma_4|^2}{1 - |\Gamma_3|^2|\Gamma_4|^2} \right]$$

$$\times \left\{ 1 - \left[|\Gamma_2|^2 + \frac{(1 - |\Gamma_2|^2)|\Gamma_1|^2}{1 - |\Gamma_1|^2|\Gamma_2|^2} \right] \left[|\Gamma_3|^2 + \frac{(1 - |\Gamma_3|^2)|\Gamma_4|^2}{1 - |\Gamma_3|^2|\Gamma_4|^2} \right] \right\}^{-1} . \quad (30)$$

Here Γ_1, Γ_2, Γ_3, and Γ_4 are the junction reflection coefficients given by the difference between the characteristic line impedances on either side of the junctions. (One should note that Eq. (30) assumes lossless lines.)

For the case of a single line between junctions 1 and 4, $\Gamma_2 = \Gamma_3 = 0$, and if we assume that these junctions are identical due to symmetry, $\Gamma_1 = \Gamma_4$. Equation (30) becomes under these conditions

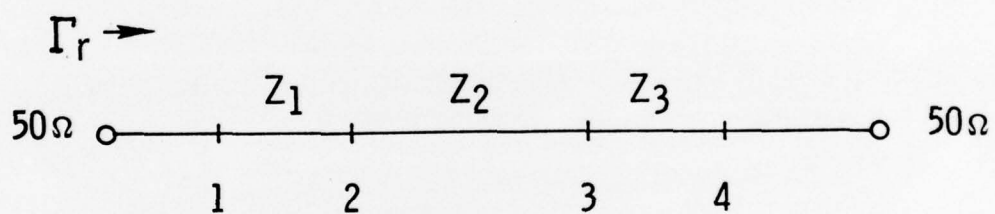$$|\Gamma_r|^2 = \frac{2|\Gamma_1|^2}{1 + |\Gamma_1|^2} . \quad (31)$$

Figure 13: Reflection coefficient Γ_r looking into a series of transmission lines with different characteristic impedances Z_1, Z_2, and Z_3, forming junctions at the points 1, 2, 3, and 4. The lines on either side of the network have $Z = 50\Omega$ lines.

In the $R = 50\Omega$ system the definition of Γ_1 leads to

$$Z = R \frac{1 + \Gamma_1}{1 - \Gamma_1} \; .$$

(32)

Combining Eqs. (31) and (32) yields

$$Z = R \frac{1 \mp \sqrt{\dfrac{P}{2 - P}}}{1 \pm \sqrt{\dfrac{P}{2 - P}}}$$

(33)

where $P = |\Gamma_r|^2$. The lower sign in Eq. (33) is for $Z > R$. By measuring the voltage standing wave ratio, Γ_r can be found as

$$|\Gamma_r|^2 = \frac{VSWR - 1}{VSWR + 1} \; .$$

(34)

Knowledge of VSWR allows one to calculate Z, or the converse.

Single microstrip lines on the substrate PBN have been fabricated and the VSWR measured for five w/H cases: w/H = 3, 2, 1, 0.6, and 0.4. Table 1 shows the experimental results (test frequency is 2.0 GHz) and the theoretically determined VSWR obtained from Eqs. (31), (32), and (34), and from Figure 8 which plots Z versus w/H based on quasi-static TEM analysis. The agreement between theory and experiment is seen to be within 10%. Improvement in the measurement procedure[7,8] should reduce the discrepancy between theory and experiment. The measurements reported here were made using an HP 8545A Automatic Network Analyzer with an HP 8500 Console System.

Table 1

VSWR for both theory (see Reference 6) and experiment for covered single microstrip on pyrolytic boron nitride.

	W/H				
	3	2	1	0.6	0.4
THEORY	1.38	1.06	1.80	2.69	2.95
EXPERIMENT	1.47	1.13	1.85	2.43	3.02
DISCREPANCY (%)	6.90	6.13	2.78	9.85	2.37

6. EXPERIMENTAL MEASUREMENTS ON COUPLED MICROSTRIP LINES ON PBN

Here we discuss the theoretical and experimental analysis leading to the fabrication of 7 dB quadrature interdigitated microstrip couplers using the anisotropic dielectric material PBN as the substrate. The importance of interdigitating the coupler will become apparent later on in this section. In order to obtain reasonable line widths w and gap spacings S between the lines, the couplers were built on H = 15 mil thick PBN substrates using n = 4 interdigitated lines. The dimensions to be discussed below are compatible with the material properties (including surface roughness and etching behavior) of PBN.

As mentioned in the Introduction, the interest in substituting PBN for a more commonly used substrate material such as alumina is that the percentage difference d between the even and odd mode phase velocities,

$$d \; = \; 100 \, \frac{v_{po} - v_{pe}}{\bar{v}} \tag{1}$$

may be made much smaller. One expects the loss in directivity due to phase velocity mismatch to go down. Degradation of the directivity due to terminal VSWR mismatch is a separate component and so the measured directivity must be taken as the lower limit on directivity improvement caused by a coupler design which reduces the d value.

Using a method of moments computer program (ANIGREEN1) employing Eq. (25) which enables microstrip coupled line parameters to be determined for anisotropic substrates under the quasi-static TEM approximation,[5] we have optimized d so that for an n = 2 structure on PBN d = 0.034%. Since the computation error is on the order of a percent or less, the w/H and S/H values corresponding to this d value (Table 2) must be interpreted as being close to the actual values for a local d zero point, and d itself taken as indicative of the fact that it can approach zeros by the proper choice of coupler parameters for PBN.

Table 2 gives w/H, S/H, B/H where B is the ground plane-to-ground plane distance for covered microstrip, the even and odd mode characteristic impedances Z_e and Z_o, the even and odd mode phase velocities v_e/c and v_o/c normalized to the speed of light c in a vacuum, the average mode phase velocity $\bar{v}/c$ normalized to c, the coupler characteristic impedance Z_c, the power coupling constant K, and d. One sees from Table 2 that for the n = 2 coupler

Table 2

Coupler parameters determined for parallel coupled microstrip on pyrolytic boron nitride employing the computer programs ANIGREEN1 and ANICOU which assume quasi-static TEM analysis for coupled lines on anisotropic dielectric substrates.

CASE	LINES	W/H	S/H	B/H	$Z_e(\Omega)$	$Z_0(\Omega)$
1	2	0.27	0.40	20	172.2	89.78
2	4	0.33	0.40	20	98.27	37.15

CASE	v_e/c	v_0/c	$\bar{v}/c$	$Z_c(\Omega)$	$K(dB)$	$d(\%)$
1	0.5948	0.5950	0.5949	124.3	10.20	0.034
2	0.5880	0.5959	0.5920	60.42	6.909	1.30

K = 10.20 dB and $Z_c = 124.3\Omega$. This Z_c value would not enable the coupler to be easily characterized experimentally with equipment calibrated to operate in a 50Ω system. In order to bring Z_c closer to 50Ω while still maintaining a low d value and a K value around 10 dB, another computer program (ANICOU) has been used. It is capable of calculating interdigitated coupled line electrical parameters for anisotropic substrates assuming equal line widths and quasi-static TEM conditions to hold. Table 2 shows the results for an $n = 4$ coupler: We see that K = 6.909 dB, d = 1.30%, and $Z_c = 60.42\Omega$. $Z_c = 60.42\Omega$ corresponds to a voltage standing wave ratio VSWR = 1.21.

This 4-line coupler has been fabricated on H = 15 mil PBN using $\lambda/4$ lines equal to 171.5 mils (the center frequency is 10.19 GHz) and its characteristics measured from 2 to 18 GHz using a Wiltron Company 610B Frequency Sweep with RF plug-ins 6219 (2-8 GHz) and 6229 (7.9-18.5 GHz), and using the HP 8425 Automatic Network Analyzer. The measured VSWR using the HP ANA is between 1.06 and 2.11 for frequencies between 2 and 12 GHz. Phase quadrature is maintained over the same frequency range within -3.9^{O} and $+2.68^{O}$. Power output from the direct (P_d), indirect (P_{id}), and isolated (P_i) coupler ports relative to a 0 dB reference are shown in Figure 14. The isolation ranges from 35.06 dB at 2 GHz to a low value of 14.31 dB at 11.250 GHz (within a 2-12 GHz interval). One sees that 7 dB $\lesssim |P_{id}| \lesssim$ 8 dB for 5.6 GHz $\lesssim$ f $\lesssim$ 14.3 GHz. P_{id} stays between 7 dB and 9 dB for 4.2 GHz $\lesssim$ f $\lesssim$ 15.7 GHz. The insertion loss L of the coupler can be determined by computing $P_L = (1 - P_d - P_{id} - P_i)$. L has a low value of 0.15 dB around 3 GHz, a high value of 1.5 dB near 12 GHz, and a value of 1.3 dB at 17 GHz.

We can conclude from the above results that it is theoretically possible to predict experimental coupled line parameters for quadrature interdigitated couplers built on anisotropic pyrolytic boron nitride. The 7 dB coupler which has been discussed demonstrates that bandwidths of over an octave with isolation over 14.3 dB can be realized for coupled structures on PBN. These results should be due in part to the low d = 1.30% value found for the phase velocity mode difference.

In order to put the above results in perspective, two other experiments were conducted: (1) 7 dB couplers using alumina and operating at a center frequency f_o equal to about 6.93 GHz were built and experimentally characterized; and (2) 7 dB couplers using PBN but operating at $f_o = 5.0$ GHz were constructed and characterized.

For a PBN 4-line coupler designed to yield the same electrical parameters as the 7 dB coupler with a $f_o = 10.2$ GHz, but with the f_o lowered to 5.0 GHz using
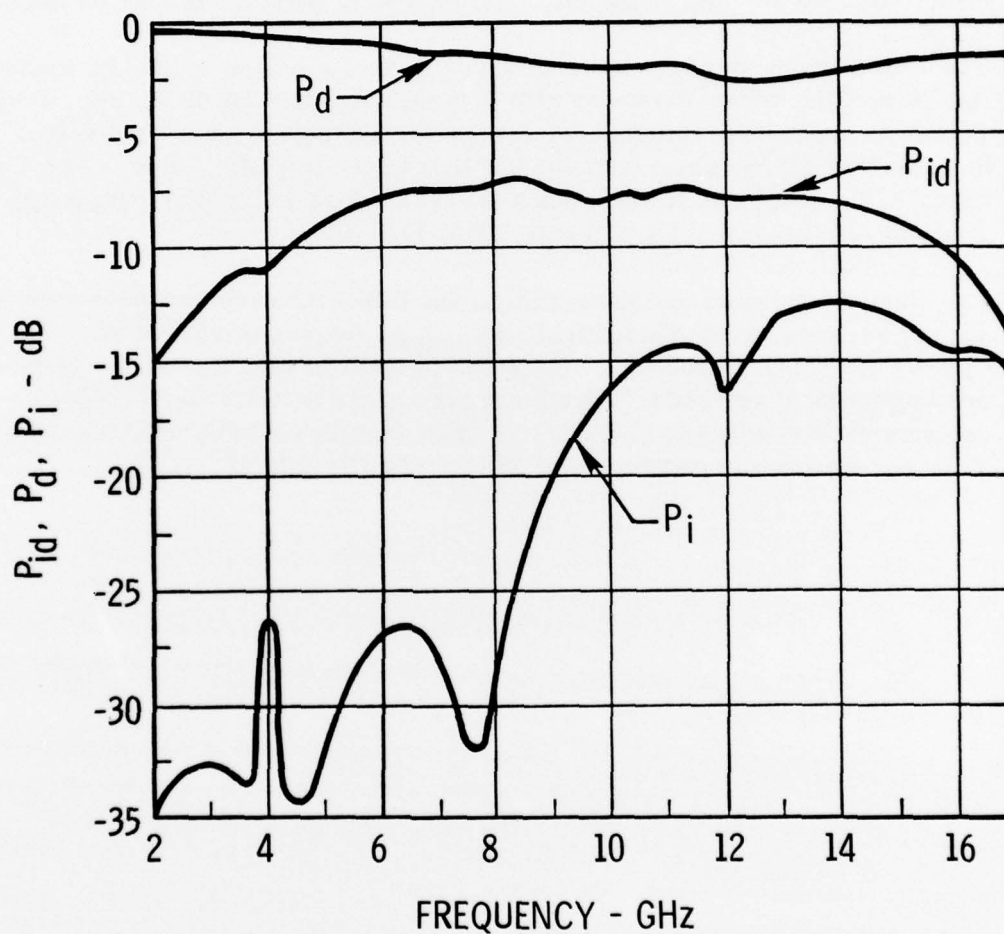
Figure 14: The direct (P_d), the coupled or indirect (P_{id}), and the isolated (P_i) output powers for the 4-line interdigitated coupler on the anisotropic dielectric substrate pyrolytic boron nitride. The coupler was designed to provide K = 7 dB of coupling (P_{id}) at the center frequency f_o = 10.19 GHz.

- 33 -

$\lambda/4$ lines equal to 349.5 mils, we obtain the results shown in Figure 15. Note that the actual etched line widths and gap spacings lead to $K = -7.34$ dB, VSWR = 1.23, and d = 1.45%. The insertion loss L is between 0.2 dB and 0.91 dB for $3.5 < f < 7.5$ GHz. For $3.15 < f < 6.15$ GHz, $7.87 < |P_{id}| < 8.25$ dB. For $1.0 < f < 9.0$ GHz, $|P_i| > 18.87$ dB. If we take $D = |P_{id} - P_i|$ as the directivity, we see that in the range $1.0 < f < 7.25$ GHz, $D > 10.62$ dB.

The 7 dB alumina couplers were designed to have a length ℓ of 171.5 mils ($f_o = 6.98$ GHz when $\lambda_o/4 = \ell$) with $K = -6.923$, $Z_c = 50.40\,\Omega$, and d = 10.8%. Figure 16 shows the experimental results for a coupler where we see that L lies between 0.1 dB and about 0.75 dB for $6.0 < f < 10.0$ GHz. For $4.0 < f < 9.2$ GHz, $8.0 < |P_{id}| < 9.15$ dB. When $3.0 < f < 12.5$ GHz, $|P_i| > 20.2$ dB. In the frequency range $3.0 < f < 9.0$ GHz, $D > 11.5$ dB.

The alumina D value is comparable to the 7 dB PBN coupler result seen in Figure 15, whereas the theoretical $d_{alumina} = 10.89\%$ compared to $d_{PBN} = 1.45\%$. This seems to imply that several factors besides d differences are important or collectively dominant over phase velocity mode dispersion in determining the values of P_i and D. Such factors could be masking the effect of using the anisotropic properties of PBN to significantly reduce d.
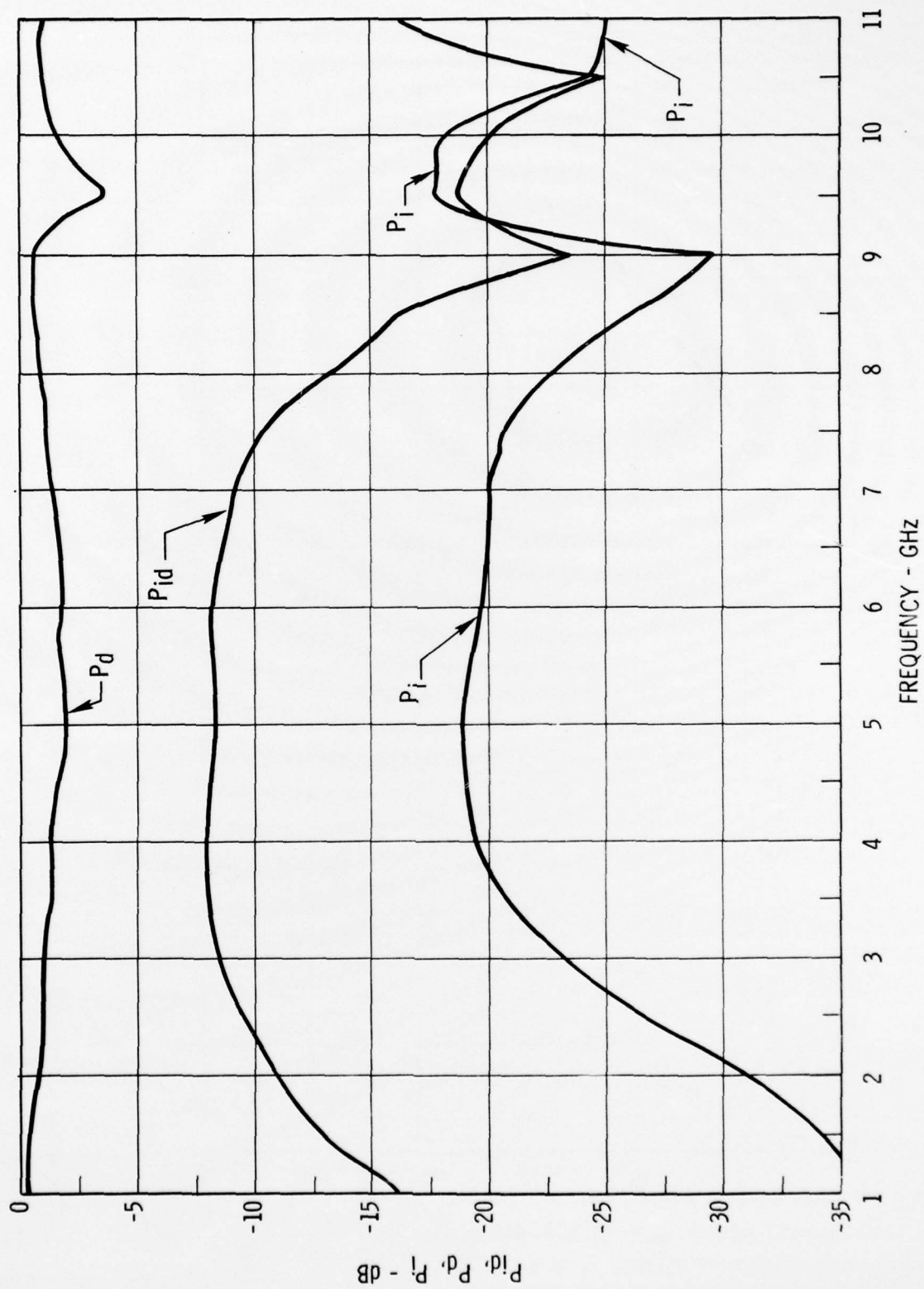
Figure 15: The output powers P_d, P_{id}, and P_i for the 4-line interdigitated coupler on the anisotropic dielectric substrate PBN. The coupler was designed to provide K = 7 dB of coupling (P_{id}) at f_o = 5.0 GHz.
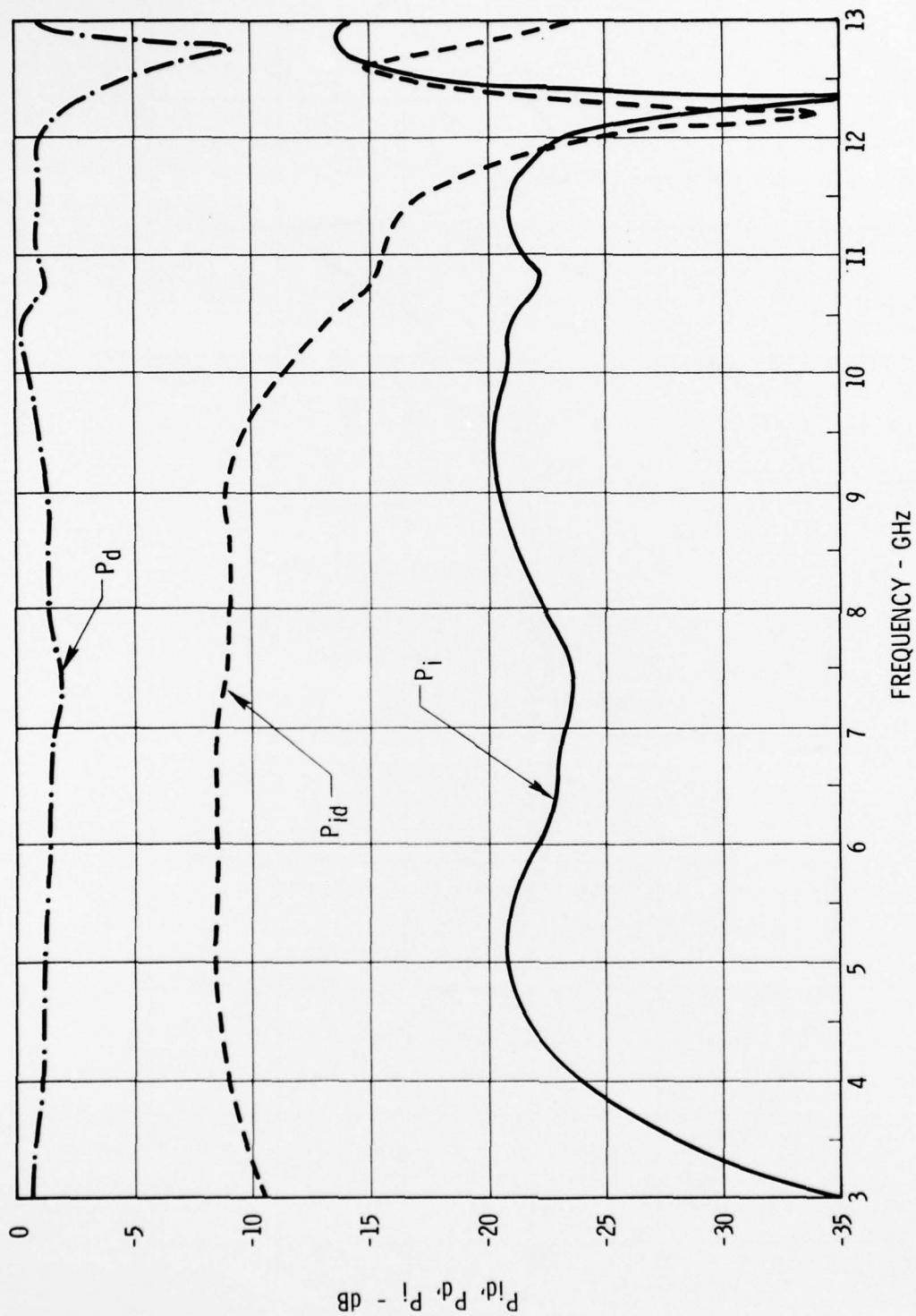
Figure 16: The output powers P_d, P_{id}, and P_i for the 4-line interdigitated coupler on the isotropic dielectric substrate alumina. The coupler was designed to provide $K = 7$ dB of coupling (P_{id}) at $f_o = 7.0$ GHz.

7. CONCLUSION

In this report we have determined the boundary conditions (B.C.) necessary to solve the problem of electromagnetic propagation in microstrip transmission lines utilizing anisotropic dielectric substrates. These B.C.'s have been used to theoretically find the Green's function relating charge on the microstrip lines to the potential around the lines. The theoretical formulation was developed to correspond to the anisotropic dielectric tensor properties of pyrolytic boron nitride (PBN) which can be obtained with two out of its three diagonal elements non-equal. The Green's function has been used in a few computer programs (ANIGREEN1, ANIGREEN2, and ANICOU) to numerically calculate by method of moments the electrical behavior of single, coupled, and interdigitated microstrip lines on PBN.

The numerical results indicate that the difference d between the even and odd mode phase velocities in coupled microstrip structures may be made very small compared to other commonly used substrates such as alumina and fused silica. By suitable choices of K and Z_c, d may be reduced by factors of five or more to values equal to 1.5% and less. One might expect the isolation in microstrip couplers fabricated on PBN to be markedly improved (P_i to decrease) due to such a low d value since the isolated power P_i is dependent on d.

The couplers built using PBN did not display this anticipated isolation (and directivity) improvement. It is felt that other material and electrical factors besides d may control the isolation performance of microstrip couplers, especially for PBN, so that a decrease in d is not unambiguously reflected in the experimental parameter measurements. Further work to clarify this problem is indicated by the experimental results.

ACKNOWLEDGMENTS

REFERENCES

1. "Boralloy; pyrolytic boron nitride", Catalogue section H-8767, Union Carbide Carbon Products, 1975.

2. R. F. Harrington, "Matrix Methods for Field Problems," Proc. IEEE, Vol. 55, No. 2, p. 136, February 1967.

3. J.A. Weiss and T.G. Bryant, "Dielectric Green's Function for Parameters of Microstrip," Electronics Letters, Vol. 6, No. 15, pp. 462-463, July 1970.

4. A. Farrar and A. T. Adams, "A Potential Theory Method for Covered Microstrip," IEEE Trans. Microwave Theory Tech. (Short Papers), Vol. MTT-21, pp. 494-496, July 1973.

5. N. G. Alexopoulos, C. Krowne and S. Kerner, "Dispersionless Coupled Microstrip Over Fused Silica-Like Anisotropic Substrates," Electronics Letters, Vol. 12, No. 22, 28th October 1976.

6. C. M. Krowne, "Microstrip Transmission Lines on Pyrolytic Boron Nitride," Electronics Letters, Vol. 12, No. 24, 25th November 1976.

7. S. O. Ajose, N. A. Mathews, and C. S. Aitchison, "Characterization of Coaxial-To-Microstrip Connector Suitable for Evaluation of Microstrip 2-Ports," Electronics Letters, Vol. 12, No. 17, August 1976.

8. W. Menzel, "Network-Analyzer Reflection Measurements of Microstrip Circuits Not Requiring Exactly Reproducible Coaxial-To-Microstrip Transitions," Electronics Letters, Vol. 12, No. 14, July 1976.

DISTRIBUTION OF FINAL REPORT

The distribution of the final report submitted in connection with this contract is as follows:

Addressee	DOAAD Code	Unclassified Unlimited
Scientific Officer	N00014	1
Administrative Contracting Officer	S0507A	1
Director, Naval Research Laboratory, Attn: Code 2627 Washington, D.C. 20375	N00173	6
Office of Naval Research Department of the Navy Arlington, Virginia 22217 Attn: Code 102IP	N00014	6
Defense Documentation Center Bldg. 5, Cameron Station Alexandria, Virginia 22314	S47031	12
Office of Naval Research Branch Office 1030 East Green Street Pasadena, Calif. 91106	N62887	1
Larry Sumney NAVALEX National Center Number 1 2511 Jefferson Davis Hwy. Arlington, Virginia 20360	8W60	1